

MNS Parameters from Neutrino Oscillations, Single Beta Decay and Double Beta Decay

K. MATSUDA, N. TAKEDA, T. FUKUYAMA,

*Department of Physics, Ritsumeikan University,
Kusatsu, Shiga 525-8577, Japan*

and

H. NISHIURA

*Department of General Education, Junior College of Osaka Institute of Technology,
Asahi-ku, Osaka 535-8585, Japan*

(Dec. 21, 2000)

Abstract

We examine the constraints on the MNS lepton mixing matrix from the present and future experimental data of the neutrino oscillation, tritium beta decay, and neutrinoless double beta decay for Majorana neutrinos. We show that the small mixing angle solutions for solar neutrino problem are disfavored for small averaged mass ($\langle m_\nu \rangle$) of neutrinoless double beta decay (≤ 0.01 eV) in the inverse neutrino mass hierarchy scenario. This is the case even in the normal mass hierarchy scenario except for very restrictive value of the averaged neutrino mass (\overline{m}_ν) of single beta decay. The lower mass bound for \overline{m}_ν is given from the present neutrino oscillation data. We obtain some relations between $\langle m_\nu \rangle$ and \overline{m}_ν . The constraints on the Majorana CP violating phases are also given.

PACS number(s): 14.60Pq. 23.40.-s 13.10.+q

Typeset using REVTeX

I. INTRODUCTION

The recent neutrino oscillation experiments [1] have shown that neutrino do indeed have masses. On the other hand, the experiments intending to determine directly neutrino mass are also on going. The upper limit of the averaged neutrino mass \overline{m}_ν defined by

$$\overline{m}_\nu^2 \equiv \sum_{j=1}^3 |U_{ej}|^2 m_j^2 \quad (1.1)$$

from the tritium β decay is 2.2 eV [2]. Here U_{aj} is the Maki-Nakagawa-Sakata (MNS) left-handed lepton mixing matrix which combines the weak eigenstate neutrino ($a = e, \mu$ and τ) with the mass eigenstate neutrino of mass m_j ($j=1,2$ and 3). The U takes the following form in the standard representation [3]:

$$U = \begin{pmatrix} c_1 c_3 & s_1 c_3 e^{i\beta} & s_3 e^{i(\rho-\phi)} \\ (-s_1 c_2 - c_1 s_2 s_3 e^{i\phi}) e^{-i\beta} & c_1 c_2 - s_1 s_2 s_3 e^{i\phi} & s_2 c_3 e^{i(\rho-\beta)} \\ (s_1 s_2 - c_1 c_2 s_3 e^{i\phi}) e^{-i\rho} & (-c_1 s_2 - s_1 c_2 s_3 e^{i\phi}) e^{-i(\rho-\beta)} & c_2 c_3 \end{pmatrix}. \quad (1.2)$$

Here $c_j = \cos \theta_j$, $s_j = \sin \theta_j$ ($\theta_1 = \theta_{12}$, $\theta_2 = \theta_{23}$, $\theta_3 = \theta_{31}$). Note that three CP violating phases, β , ρ and ϕ appear in U for Majorana particles [4]. On the other hand, the most recent experimental upper bound for the averaged mass $\langle m_\nu \rangle$ defined by

$$\langle m_\nu \rangle \equiv \left| \sum_{j=1}^3 U_{ej}^2 m_j \right| \quad (1.3)$$

for Majorana neutrinos from the neutrinoless double beta decay $((\beta\beta)_{0\nu})$ is given by $\langle m_\nu \rangle < 0.2$ eV in the absence of right-handed lepton current [5]. The next generation experiments such as GENIUS [6], CUORE [7], MOON [8] are anticipated to reach a considerably more stringent limit $\langle m_\nu \rangle < 0.01 - 0.001$ eV. In these situations it is necessary to confine the MNS parameters and the Majorana phases by incorporating all these direct and indirect experiments. To disentangle the complicated correlations among the data from many different kinds of experiments, we proposed a graphical method [9] [10]. This method enables us to grasp the geometrical relations among the parameters of masses, mixing angles,

CP phases etc. and obtain the constraints on them more easily than the analytical calculations [3] [11] [12]. In this work we apply this method to obtain the constraints on the MNS parameters by using the neutrino oscillation, $(\beta\beta)_{0\nu}$ and single beta decay experiments.

This article is organized as follows. In section 2 we review the graphical representations of the complex masses and the CP violating phases appeared in $\langle m_\nu \rangle$. In section 3 we discuss the constraints among mixing angles, $\langle m_\nu \rangle$ and \overline{m}_ν from $(\beta\beta)_{0\nu}$, single beta decay and neutrino oscillation. In section 4 we give the allowed region in the $\langle m_\nu \rangle$ - \overline{m}_ν plane, first irrespective and second respective of the mixing angles. Constraints on the CP violating phases are discussed in section 5. Section 6 is devoted to summary.

II. GRAPHICAL REPRESENTATIONS OF THE COMPLEX MASSES AND THE CP VIOLATING PHASES APPEARING IN NEUTRINOLESS DOUBLE BETA DECAY

Let us review our graphical representations of the complex mass and the CP violating phases appeared in $(\beta\beta)_{0\nu}$, which are proposed in [9] [10]. The averaged mass $\langle m_\nu \rangle$ of Eq.(1.3) [13] is the absolute value of averaged complex masses for Majorana neutrinos,

$$\langle m_\nu \rangle = |M_{ee}|, \quad (2.1)$$

where the averaged complex mass M_{ee} is, after suitable phase convention, defined by

$$M_{ee} \equiv \sum_{j=1}^3 U_{ej}^2 m_j \equiv \sum_{j=1}^3 |U_{ej}|^2 \widetilde{m}_j. \quad (2.2)$$

Here we have defined the complex masses $\widetilde{m}_i (i = 1, 2 \text{ and } 3)$ by

$$\begin{aligned} \widetilde{m}_1 &\equiv m_1, & \widetilde{m}_2 &\equiv e^{2i\beta} m_2, \\ \widetilde{m}_3 &\equiv e^{2i(\rho-\phi)} m_3 \equiv e^{2i\rho'} m_3. \end{aligned} \quad (2.3)$$

Since $\sum_{j=1}^3 |U_{ej}|^2 = 1$, the position of M_{ee} in a complex mass plane is within the triangle formed by the three vertices $\widetilde{m}_i (i = 1, 2 \text{ and } 3)$ if the magnitudes of $|U_{ej}|^2 (j = 1, 2 \text{ and } 3)$

are unknown (Fig.1). This triangle is referred to the complex-mass triangle [9] [10]. The three mixing matrix elements $|U_{ej}|^2$ ($j = 1, 2$ and 3) indicate the division ratios for the three portions of each side of the triangle which are divided by the parallel lines to the side lines of the triangle passing through the M_{ee} (Fig.2). The CP violating phases 2β and $2\rho'$ represent the rotation angles of \widetilde{m}_2 and \widetilde{m}_3 around the origin, respectively. Since $\langle m_\nu \rangle = |M_{ee}|$, the present experimental upper bound on $\langle m_\nu \rangle$ (we denote it $\langle m_\nu \rangle_{max}$) indicates the maximal distance of the point M_{ee} from the origin and forms the circle in the complex plane (Fig.1).

III. CONSTRAINTS ON MIXING ANGLES FROM NEUTRINO OSCILLATIONS, NEUTRINOLESS DOUBLE BETA AND SINGLE BETA DECAYS

We first discuss the constraints on the mixing angles from $(\beta\beta)_{0\nu}$ and neutrino oscillations. The averaged mass $\langle m_\nu \rangle$ obtained from $(\beta\beta)_{0\nu}$ is given by the absolute value of averaged complex mass M_{ee} as in Eq.(2.2). The CP phases β and ρ' in M_{ee} may have still time to be determined. Let us move these two parameters freely and find constraints irrespective of these phases. It goes from Eq.(2.2) that

$$|M_{ee} - |U_{e1}|^2 \widetilde{m}_1| = ||U_{e2}|^2 \widetilde{m}_2 + |U_{e3}|^2 \widetilde{m}_3|. \quad (3.1)$$

Hence one finds

$$||U_{e2}|^2 m_2 - |U_{e3}|^2 m_3| \leq |M_{ee} - |U_{e1}|^2 m_1| \leq |U_{e2}|^2 m_2 + |U_{e3}|^2 m_3. \quad (3.2)$$

Therefore, the position of M_{ee} in a complex mass plane is within the annulus shown in Fig.3.

As we mentioned, M_{ee} must also be inside of the circle with radius $\langle m_\nu \rangle_{max}$.

So we obtain the consistency condition

$$\begin{aligned} -\langle m_\nu \rangle_{max} &< |U_{e1}|^2 m_1 - ||U_{e2}|^2 m_2 - |U_{e3}|^2 m_3| \equiv a_+ \\ &\text{and} \\ a_- &\equiv |U_{e1}|^2 m_1 - |U_{e2}|^2 m_2 - |U_{e3}|^2 m_3 < \langle m_\nu \rangle_{max}. \end{aligned} \quad (3.3)$$

In order to obtain the constraints on the parameters from the consistency condition(3.3) let us use, instead of m_1 , m_2 and m_3 , $\overline{m_\nu}$, $\Delta m_{12}^2 \equiv m_2^2 - m_1^2$ and $\Delta m_{23}^2 \equiv m_3^2 - m_2^2$ which are measurable in single beta decay or neutrino oscillation experiments. Namely, by inserting the relations

$$m_2 = \sqrt{m_1^2 + \Delta m_{12}^2}, \quad (3.4)$$

$$m_3 = \sqrt{m_2^2 + \Delta m_{23}^2} = \sqrt{m_1^2 + \Delta m_{12}^2 + \Delta m_{23}^2} \quad (3.5)$$

into Eq.(1.1) with the unitarity condition that $|U_{e2}|^2 = 1 - |U_{e1}|^2 - |U_{e3}|^2$, we obtain the following expressions for m_1 , m_2 , and m_3 [14]:

$$m_1 = \sqrt{\overline{m_\nu}^2 - (1 - |U_{e1}|^2)\Delta m_{12}^2 - |U_{e3}|^2\Delta m_{23}^2}, \quad (3.6)$$

$$m_2 = \sqrt{\overline{m_\nu}^2 + |U_{e1}|^2\Delta m_{12}^2 - |U_{e3}|^2\Delta m_{23}^2}, \quad (3.7)$$

$$m_3 = \sqrt{\overline{m_\nu}^2 + |U_{e1}|^2\Delta m_{12}^2 + (1 - |U_{e3}|^2)\Delta m_{23}^2}. \quad (3.8)$$

It should be noted from $0 \leq m_1^2$ that the neutrino mass $\overline{m_\nu}$ in Eq.(1.1) is predicted to have lower bound as

$$\sqrt{(1 - |U_{e1}|^2)\Delta m_{12}^2 + |U_{e3}|^2\Delta m_{23}^2} \leq \overline{m_\nu}. \quad (3.9)$$

Now we discuss constraints among MNS mixing parameters $|U_{e1}|^2$, $|U_{e3}|^2$, averaged neutrino masses $\overline{m_\nu}$, and $\langle m_\nu \rangle$ from the consistency condition (3.3) by using the data obtained from the neutrino oscillation experiments. In the following discussions we consider two scenarios for neutrino mass hierarchy:

(A) normal mass hierarchy where $m_1 \sim m_2 \ll m_3$ and

(B) inverse mass hierarchy where $m_1 \ll m_2 \sim m_3$.

For the case (A), we have

$$\Delta m_{23}^2 = \Delta m_{atm}^2 \cong 0.0032 \text{ eV}^2 \quad (3.10)$$

from the Super-Kamiokande atmospheric neutrino oscillation experiment [1]. For the solar neutrino deficit [15] we have

$$\Delta m_{12(MSW)}^2 = \Delta m_{solar(MSW)}^2 \cong 0.00001 \text{ eV}^2 \quad (3.11)$$

for MSW solutions and

$$\Delta m_{12(Just\ So)}^2 = \Delta m_{solar(Just\ So)}^2 \cong 4.3 \times 10^{-10} \text{ eV}^2 \quad (3.12)$$

for vacuum oscillation (Just So) solution. From the recent CHOOZ reactor experiment [16] we have

$$|U_{e3}|^2 < 0.03. \quad (3.13)$$

So two averaged masses $\overline{m_\nu}$, $\langle m_\nu \rangle$ and $|U_{e1}|^2$ are left as free parameters. The $|U_{ei}|^2$ runs over the large mixing angle (LMA-MSW) and the small mixing angle (SMA-MSW) solutions to the solar neutrino problem.

For the case (B), we may simply exchange the suffix 1 for 3 in the arguments of normal mass hierarchy. That is, Eqs.(3.10)-(3.13) are replaced by

$$\Delta m_{12}^2 = \Delta m_{atm}^2 \cong 0.0032 \text{ eV}^2, \quad (3.14)$$

$$\Delta m_{23(MSW)}^2 = \Delta m_{solar(MSW)}^2 \cong 0.00001 \text{ eV}^2, \quad (3.15)$$

$$\Delta m_{23(Just\ So)}^2 = \Delta m_{solar(Just\ So)}^2 \cong 4.3 \times 10^{-10} \text{ eV}^2, \quad (3.16)$$

$$|U_{e1}|^2 < 0.03, \quad (3.17)$$

respectively. So in this case $|U_{e3}|^2$ in place of $|U_{e1}|^2$ together with two averaged masses are left unknown.

Substituting the observed values in oscillation experiments into Eq.(3.3), we obtain the constraints on the two averaged masses as well as $|U_{e1}|^2$ for the normal mass hierarchy and $|U_{e3}|^2$ for the inverse mass hierarchy (Fig.4). Here we have set the typical values for $\langle m_\nu \rangle_{max}$. So the allowed regions are given in the $\overline{m_\nu}$ - $|U_{e1}|^2$ plane for fixed values of $\langle m_\nu \rangle_{max}$, Δm_{solar}^2 , Δm_{atm}^2 , and $|U_{e3}|^2$ in the normal mass hierarchy scenario (Eqs.(3.10)-(3.13)), and are given in the $\overline{m_\nu}$ - $|U_{e3}|^2$ plane for fixed values of $\langle m_\nu \rangle_{max}$, Δm_{solar}^2 , Δm_{atm}^2 , and $|U_{e1}|^2$

in the inverse mass hierarchy scenario (Eqs.(3.14)-(3.17)). It is seen from Fig.4 that, for small $\langle m_\nu \rangle_{max}$, the SMA-MSW solution to the solar neutrino problems is disfavored for both hierarchies. That is, the SMA-MSW is allowed only in the very narrow region; in the normal mass hierarchy $\overline{m}_\nu \sim 1 \times 10^{-2}$ eV for $\langle m_\nu \rangle_{max} < 0.01$ eV and in the inverse mass hierarchy $\overline{m}_\nu \sim 1 \times 10^{-1}$ eV for $\langle m_\nu \rangle_{max} < 0.1$ eV. If $\langle m_\nu \rangle_{max} < 0.01$ eV, the SMA-MSW in the inverse mass hierarchy is excluded irrespective of \overline{m}_ν . These values of $\langle m_\nu \rangle_{max}$ are very marginal to the present experimental values and, therefore, the future experiments such as GENIUS [6], CUORE [7], MOON [8] will play important roles for choosing the neutrino mass hierarchy scenarios. Klapdor et al. have discussed about the same subjects in excellent clearness [17]. We have developed the graphical method, incorporated \overline{m}_ν in the analyses and obtained more stringent constraints than those in [17]. As for \overline{m}_ν , it seems very hard to improve the upper limit beyond the present 3eV to 0.5eV [2]. It needs the improvement of the intensity of source or the acceptance of spectrometer by factor 100-1000. Also the problem of $\overline{m}_\nu^2 < 0$ still remains unsolved [18]. Anyhow, however, if non zero \overline{m}_ν is measured in the neighborhood of the present upper limit, then it immediately leads to the LMA-MSW or Just So solution and the impacts to the other branches are very large. Theoretical upper bound of neutrino masses, for instance, from the matching condition for fluctuation powers at the COBE scale and at the cluster scale for generous parameter space is 0.9eV [19]. The Fig.4 also shows that \overline{m}_ν is larger than $O(10^{-2})$ eV for the normal neutrino mass hierarchy scenario and than $O(10^{-1})$ eV for the inverse neutrino mass hierarchy scenario irrespective of $\langle m_\nu \rangle_{max}$, which comes from Eq.(3.9). If the GENIUS I and II can not observe the $(\beta\beta)_{0\nu}$ for $\langle m_\nu \rangle \gtrsim 0.01$ eV and if LMA-MSW and Just So solutions become disfavored, then the normal neutrino mass hierarchy scenario (each lower three panels of (a) and (b) in Fig.4) can survive.

IV. CONSTRAINTS ON AVERAGED NEUTRINO MASSES DEFINED IN NEUTRINOLESS DOUBLE BETA DECAY AND IN SINGLE BETA DECAY

We will show how the data of \overline{m}_ν give the restriction on the complex mass triangle of the $(\beta\beta)_{0\nu}$. By using Eq.(1.1) and the unitarity condition of U_{ei} , one finds that among three mixing matrix elements $|U_{ej}|$ ($j = 1, 2$ and 3) only one matrix element is free parameter and the others are expressed in terms of it once neutrino masses m_i and \overline{m}_ν are fixed:

$$\begin{aligned} |U_{e1}|^2 &= \frac{m_3^2 - \overline{m}_\nu^2 - |U_{e2}|^2(m_3^2 - m_2^2)}{m_3^2 - m_1^2}, \\ |U_{e3}|^2 &= \frac{\overline{m}_\nu^2 - m_1^2 - |U_{e2}|^2(m_2^2 - m_1^2)}{m_3^2 - m_1^2}. \end{aligned} \quad (4.1)$$

Let us assume that the averaged mass in tritium beta decay has the definite value \overline{m}_ν . Then it goes from Eqs.(1.1), (4.1) and Fig.2 that the position of M_{ee} is restricted to be on the line segment AB in Fig.5(a) for the case $\overline{m}_\nu < m_2$ or $A'B$ in Fig.5(b) for the case $\overline{m}_\nu > m_2$. Here from the condition $0 \leq |U_{ei}|^2 \leq 1$ ($i = 1, 2$ and 3), the mixing matrix elements $|U_{ei}|$ range over

$$\begin{aligned} \frac{m_2^2 - \overline{m}_\nu^2}{m_2^2 - m_1^2} &\leq |U_{e1}|^2 \leq \frac{m_3^2 - \overline{m}_\nu^2}{m_3^2 - m_1^2}, \\ \frac{\overline{m}_\nu^2 - m_1^2}{m_2^2 - m_1^2} &\geq |U_{e2}|^2 \geq 0, \\ 0 &\leq |U_{e3}|^2 \leq \frac{\overline{m}_\nu^2 - m_1^2}{m_3^2 - m_1^2} \end{aligned} \quad (4.2)$$

for the case $\overline{m}_\nu < m_2$ and

$$\begin{aligned} 0 &\leq |U_{e1}|^2 \leq \frac{m_3^2 - \overline{m}_\nu^2}{m_3^2 - m_1^2}, \\ \frac{m_3^2 - \overline{m}_\nu^2}{m_3^2 - m_2^2} &\geq |U_{e2}|^2 \geq 0, \\ \frac{\overline{m}_\nu^2 - m_2^2}{m_3^2 - m_2^2} &\leq |U_{e3}|^2 \leq \frac{\overline{m}_\nu^2 - m_1^2}{m_3^2 - m_1^2} \end{aligned} \quad (4.3)$$

for the case $\overline{m}_\nu > m_2$. Eq.(4.1) combined with the analysis of the $(\beta\beta)_{0\nu}$ gives additional constraints on the position of the complex mass M_{ee} as follows.

The M_{ee} runs over the line segments with free parameter U_{e2} for fixed β, ρ' . (Observed data of U_{ei} will be incorporated later in this section.) Here A divides the line $\overline{m_1 m_2}$ by $Am_1 : A\overline{m_2} = r : s$. The r and s are defined by

$$r = \frac{\overline{m_\nu}^2 - m_1^2}{m_2^2 - m_1^2}, \quad s = \frac{m_2^2 - \overline{m_\nu}^2}{m_2^2 - m_1^2} \quad (r + s = 1). \quad (4.4)$$

Therefore

$$OA = rm_2 e^{2i\beta} + sm_1. \quad (4.5)$$

Hence if we move β freely, the position A occupies a circle (dotted circle crossing at A_\pm with horizontal axis (Fig.6(a)). Likewise, B divides the line $\overline{m_1 m_3}$ by $Bm_1 : B\overline{m_3} = q : p$, where p and q are defined by

$$p = \frac{m_3^2 - \overline{m_\nu}^2}{m_3^2 - m_1^2}, \quad q = \frac{\overline{m_\nu}^2 - m_1^2}{m_3^2 - m_1^2} \quad (p + q = 1). \quad (4.6)$$

So OB is given by

$$OB = qm_3 e^{2i\rho'} + pm_1. \quad (4.7)$$

Then if we move ρ' freely, the position B occupies a circle (dotted circle crossing at B_\pm with horizontal axis (Fig.6(a))). Thus making both β and ρ' run freely, M_{ee} on the line segments is inside an larger circle, the region bounded by dotted circles passing $A_- AA_+$ (Fig.6). The A_\pm and B_\pm are easily obtained graphically. For instance, A_- divides $\overline{(-m_2)m_1}$ as $\overline{(-m_2)A_-} : \overline{A_- m_1} = \overline{m_2 A} : \overline{A m_1} = s : r$, where use has been made of the ratio in Fig.5. The other points are also obtained analogously. Thus we easily obtain graphically

$$\text{Max}\{\overline{OA_-}, 0\} = \text{Max}\left\{\frac{m_1 m_2 - \overline{m_\nu}^2}{m_2 - m_1}, 0\right\} \leq \langle m_\nu \rangle \leq \overline{OA_+} = \frac{m_1 m_2 + \overline{m_\nu}^2}{m_2 + m_1} \quad (4.8)$$

for the case $\overline{m_\nu} \leq m_2$. The $\text{Max}\{a, b\}$ indicates the larger value between a and b . As for the case of $\overline{m_\nu} > m_2$ (Fig.6(b)), we repeat the almost same arguments and obtain

$$\text{Max}\{\overline{OA_-}, 0\} = \text{Max}\left\{\frac{\overline{m_\nu}^2 - m_3 m_2}{m_3 - m_2}, 0\right\} \leq \langle m_\nu \rangle \leq \overline{OA_+} = \frac{m_3 m_2 + \overline{m_\nu}^2}{m_3 + m_2}. \quad (4.9)$$

Note that Eq.(4.9) is obtained from Eq.(4.8) by exchanging the suffix 3 for 1. Summing up the results of Eqs.(4.8) and (4.9), we obtain the allowed region in the $\langle m_\nu \rangle - \overline{m}_\nu$ plane (Fig.7). In this Figure we have not specified the points on the segments AB or $A'B$ which means that the information of mixing angles are smeared out. The m_1 is only free parameter and the other masses are expressed in terms of Δm_{12}^2 and Δm_{23}^2 from Eqs.(3.4) and (3.5). If we incorporate the information of the mixing angles (some restricted regions), the points on the segments AB or $A'B$ in Fig.6 are not specified but restricted in some small region and we have more stringent constraints in the $\langle m_\nu \rangle - \overline{m}_\nu$ plane than in Fig.7. We list only the cases of LMA-MSW and SMA-MSW solutions in the normal mass hierarchy (Fig.8), where we have adopted $|U_{e3}|^2 < 0.03$, and $0.3 < |U_{e2}|^2 < 0.7$ for LMA-MSW and $1 \times 10^{-3} < |U_{e2}|^2 < 1 \times 10^{-2}$ for SMA-MSW. The first, second and third row panels correspond to the case $m_1 = 10^{-5}\text{eV}$, 10^{-3}eV , and 10^{-1}eV , respectively. Namely within these conditions of $|U_{ei}|^2$, all masses are fixed and CP phases are free parameters in each panel. From Fig.8(f), if GENIUS I gives a new upper bound on $\langle m_\nu \rangle$, SMA-MSW with $m_1 \sim 10^{-1}\text{eV}$ is excluded. This figure is rather useful for checking models which predict mass spectrum.

V. CONSTRAINTS ON CP VIOLATING PHASES FROM NEUTRINOLESS DOUBLE BETA AND SINGLE BETA DECAYS

Now we discuss possible constraints on CP violating phases [9] [10] [20] from $(\beta\beta)_{0\nu}$ and single beta decay experiments. First, we consider the constraints for the typical values of the mixing matrix element such as (i) $|U_{e3}|^2 = 0$, minimum value of $|U_{e3}|^2$, and (ii) $|U_{e3}|^2 = \frac{\overline{m}_\nu^2 - m_1^2}{m_3^2 - m_1^2}$, maximum value of $|U_{e3}|^2$, in the case where $\overline{m}_\nu < m_2$. That is, if m_i ($i = 1, 2$ and 3), \overline{m}_ν , and U_{e3} are given, then U_{ej} ($j = 1, 2$) are also given from Eq.(4.1). Hence if we impose the observed $\langle m_\nu \rangle_{max}$, then we can constrain the CP violating phases.

For the case $|U_{e3}|^2 = 0$, the position of complex mass M_{ee} is restricted to be at point A in Fig.5(a) as was discussed in section 4. Therefore, when we change the CP violating phase β , M_{ee} moves along a circle passing A_-AA_+ (Fig.6) Since this circle must be inside

of the circle with the radius $\langle m_\nu \rangle_{max}$. Two these circles intersect at β satisfying \overline{OA} of Eq.(4.5) = $\langle m_\nu \rangle_{max}$, that is,

$$\cos^{-1} \frac{\langle m_\nu \rangle_{max}^2 - (m_1 r)^2 - (m_2 s)^2}{2m_1 m_2 r s} \leq |2\beta| \leq \pi \quad (5.1)$$

for the case $\frac{m_1 m_2 - \overline{m}_\nu^2}{m_2 - m_1} \leq \langle m_\nu \rangle_{max} \leq \frac{m_1 m_2 + \overline{m}_\nu^2}{m_2 + m_1}$, where r and s are defined in Eq.(4.4). We have no constraint on β for the case $\frac{m_1 m_2 + \overline{m}_\nu^2}{m_2 + m_1} \leq \langle m_\nu \rangle_{max}$ and the case $\langle m_\nu \rangle_{max} \leq -\frac{m_1 m_2 - \overline{m}_\nu^2}{m_2 - m_1}$ is excluded.

For the case $|U_{e3}|^2 = \frac{\overline{m}_\nu^2 - m_1^2}{m_3^2 - m_1^2}$, the position of complex mass M_{ee} is restricted to be at point B in Fig.5(a). Therefore, when we change the CP violating phase ρ' , M_{ee} moves along a circle B_-BB_+ (Fig.6) irrespective of the CP violating phase β . Thus we obtain the allowed bounds on the CP violating phase ρ' ,

$$\cos^{-1} \frac{\langle m_\nu \rangle_{max}^2 - (m_1 p)^2 - (m_3 q)^2}{2m_1 m_3 p q} \leq |2\rho'| \leq \pi \quad (5.2)$$

for the case $\frac{m_1 m_3 - \overline{m}_\nu^2}{m_3 - m_1} \leq \langle m_\nu \rangle_{max} \leq \frac{m_1 m_3 + \overline{m}_\nu^2}{m_3 + m_1}$, where p and q are defined in Eq.(4.6). We have no constraint on ρ' for the case $\frac{m_1 m_3 + \overline{m}_\nu^2}{m_3 + m_1} \leq \langle m_\nu \rangle_{max}$ and the case $\langle m_\nu \rangle_{max} \leq -\frac{m_1 m_3 - \overline{m}_\nu^2}{m_3 - m_1}$ is excluded. The case for $\overline{m}_\nu > m_2$ can be discussed in the same way.

So far we have considered the special limit of mixing angles and smeared one CP phases. In what follows, we consider the constraints on both two CP phases by incorporating mixing angles by use of Fig.2 and Fig.5. We obtain the allowed region among \overline{m}_ν , CP violating phases β and ρ' for the LMA-MSW solution in the normal and inverse mass hierarchy scenarios. It is given in Fig.9 and Fig.10 in the case where the e - μ mixing is nearly maximal, namely $|U_{e1}|^2 \simeq |U_{e2}|^2 \simeq 1/2$. In these figures, let us consider the situation that $\langle m_\nu \rangle$ and \overline{m}_ν have the nonzero values in the neighborhood of the present or near future upper limits. For the case of $|U_{e3}|^2 \ll O(10^{-2})$, one obtains the restriction on β only by any experiments because Eq.(5.1) is irrespective of ρ' . However, if $|U_{e3}|^2$ has a slight non-zero value ($|U_{e3}|^2 = O(10^{-2})$) and if GENIUS II first finds a nonzero $\langle m_\nu \rangle$, then one obtains the restrictions on not only β but also ρ' ((b) and (d) in Fig.9 and Fig.10). However β and ρ' are very sensitive to the value in the neighborhood of $|U_{e2}|^2 \simeq 1/2$. Fig.9 is the case for

$|U_{e2}|^2 = 0.5$. In this case, $\sin \rho' \ll 1$ and $\sin \beta \simeq 1$ both in the normal (Fig.9 (b)) and inverse (Fig.9 (d)) hierarchy scenarios. The case for $|U_{e2}|^2 = 0.47$ is given in Fig.10. In this case, $\sin \beta \simeq 1$ and $\sin \rho' \simeq 1$ in the normal hierarchy (Fig.10 (b)) and $\sin \beta \ll 1$ and $\sin \rho' \simeq 1$ in the inverse hierarchy (Fig.10 (d)). In these figures, nevertheless, the restrictions of β in the normal hierarchy ($\sin \beta \simeq 1$) and of $|\rho' - \beta|$ in the inverse hierarchy ($\sin |\beta - \rho'| \simeq 1$) are insensitive to $|U_{e2}|^2 \simeq 1/2$.

VI. SUMMARY

In addition to the neutrino oscillation experiments, the experiments intending to determine directly neutrino mass, such as neutrinoless double beta decay experiments (GENIUS, CUORE, MOON etc.), and the tritium beta decay experiments (Mainz, Troitsk etc.) are on going and anticipated to reach a considerably more stringent limit. In these situations, it is more and more important to consider MNS parameters from various experiments and phenomena. In this paper, assuming that neutrinos are Majorana particles of three generations, we have examined the constraints on the mixing angles and Majorana CP violating phases of the MNS lepton mixing matrix by analyzing $(\beta\beta)_{0\nu}$ together with the neutrino oscillations and the single beta decay. In this analysis we have seriously considered the CP violating phases appeared in $(\beta\beta)_{0\nu}$ and applied the graphical method proposed in the previous papers (Fig.1 and 2). The meaning of incorporating CP phases is twofold. One is, of course, to predict their magnitudes. The other is to extract the results which are valid irrespective of the magnitudes of CP phases. Sections 3 and 4 correspond to the latter case and section 5 to the former case.

Our results are in order:

(i) By changing the CP violating phases freely we have discussed the consistency condition among the neutrinoless double beta decay and neutrino oscillations for the two hierarchy scenarios of neutrino masses (normal and inverse mass hierarchies). In this analysis we have used only observable neutrino mass parameters such as $\langle m_\nu \rangle$, \overline{m}_ν , Δm_{12}^2 , and Δm_{23}^2 instead

of using m_1 , m_2 , and m_3 by incorporating the single beta decay also. It should be noted that m_1 , m_2 , and m_3 are related to the observable parameters as seen in Eqs.(3.6)-(3.8). Then, we find that SMA-MSW for the solar neutrino problem are disfavored for small $\langle m_\nu \rangle$ (≤ 0.01 eV) in the inverse neutrino mass hierarchy scenario. This is the case even in the normal mass hierarchy scenario except for very restrictive value of $\overline{m}_\nu \sim 1 \times 10^{-2}$ eV. In addition to this, we have also found that the neutrino mass observed in the single beta decay \overline{m}_ν is predicted to be larger than $O(10^{-2})$ eV for the normal neutrino mass hierarchy scenario and than $O(10^{-1})$ eV for the inverse neutrino mass hierarchy scenario. Those results are shown in Fig.4.

(ii) We have discussed the allowed region in the two neutrino masses plane, $\langle m_\nu \rangle$ and \overline{m}_ν which are observable in $(\beta\beta)_{0\nu}$ and single beta decay respectively. First we have obtained Eqs.(4.8) and (4.9) which are irrelevant to the mixing angles (Fig.7). Then more stringent constraints are obtained by incorporating the data of mixing angles (Fig.8).

(iii) We have analytically obtained the constraints, Eqs.(5.1) and (5.2), on the Majorana CP violating phases for typical limits of mixing angle with use of the observable neutrino masses ($\langle m_\nu \rangle$ and \overline{m}_ν). The m_1 , m_2 , and m_3 in these constraints are described in terms of observables using Eqs.(3.6)-(3.8). Then we have obtained the relations among the CP phases and \overline{m}_ν for several possible values of $\langle m_\nu \rangle$, $|U_{e2}|^2$ with fixed Δm_{solar}^2 and Δm_{atm}^2 , and $|U_{e3}|^2$. For the case of $|U_{e1}|^2 \simeq |U_{e1}|^2 \simeq 1/2$, CP phases are severely constrained if $\langle m_\nu \rangle$ and \overline{m}_ν have nonzero values in the neighborhood of the present experimental upper limits (Fig.9 and Fig.10).

We are grateful to T. Ohshima for comments. The work of K.M. is supported by the JSPS Research Fellowship, No.10421.

REFERENCES

- [1] T.Kajita, talk presented at Neutrino '98 (Takayama, Japan, June 1998). H. Sobel, talk presented at Neutrino 2000 (Sudbury, Canada, June 2000).
- [2] Ch. Weinheimer et al., Phys. Lett. **B460** 219 (1999); V.M. Lobashev et al., Phys. Lett. **B460** 227 (1999); Particle Data Group, Eur. Phys. J. **C15** 1 (2000); C. Weinheimer, talk presented at Neutrino 2000 (Sudbury, Canada, June 2000); V.M. Lobashev, talk presented at Neutrino 2000 (Sudbury, Canada, June 2000).
- [3] T. Fukuyama, K. Matsuda, and H. Nishiura, Phys. Rev. **D57** 5844 (1998).
- [4] S.M. Bilenky, J. Hosek and S.T. Petcov, Phys. Lett. **94B** 495 (1980); J. Schechter and J.W.F. Valle, Phys. Rev. **D22** 2227 (1980); M. Doi, T. Kotani, H. Nishiura, K. Okuda and E. Takasugi, Phys. Lett. **102B** 323 (1981); A. Barroso and J. Maalampi, Phys. Lett. **132B** 355 (1983).
- [5] L. Baudis et al., Phys. Rev. Lett. **83** 41 (1999).
- [6] J. Hellmig, H.V. Klapdor-Kleingrothaus, Z.Phys. **A 359** 361 (1997); H.V. Klapdor-Kleingrothaus, M. Hirsch, Z.Phys. **A 359** 382 (1997); L. Baudis et al., Phys. Rep. **307** 301 (1998).
- [7] E. Fiorini et al., Phys. Rep. **307** 309 (1998).
- [8] H. Ejiri et al., nucl-ex/9911008.
- [9] K. Matsuda, N. Takeda, T. Fukuyama, and H. Nishiura, Phys. Rev. **D62**, 093001 (2000).
- [10] K. Matsuda, N. Takeda, T. Fukuyama, and H. Nishiura, to appear in Phys. Rev. D (hep-ph/0007237).
- [11] T. Fukuyama, K. Matsuda, and H. Nishiura, Mod. Phys. Lett. **A13** 2279 (1998).
- [12] H. Nishiura, K. Matsuda, and T. Fukuyama, Mod. Phys. Lett. **A14** 433 (1999).

- [13] M. Doi, T. Kotani, H. Nishiura, K. Okuda and E. Takasugi, Phys. Lett. **102B** 323 (1981); M. Doi, T. Kotani and E. Takasugi, Prog. Theor. Phys. Suppl. **83** 1 (1985); W.C. Haxton and G.J. Stophenson Jr., Prog. Part. Nucl. Phys. **12** 409 (1984).
- [14] K. Matsuda, N. Takeda, T. Fukuyama, and H. Nishiura, Proceeding of ICHEP 2000 (World Scientific)
- [15] Y. Suzuki, talk presented at Neutrino 2000 (Sudbury, Canada, June 2000); V. Gavrin, talk presented at Neutrino 2000 (Sudbury, Canada, June 2000); K. Lande, talk presented at Neutrino 2000 (Sudbury, Canada, June 2000); K. Hirata et al., Phys. Rev. Lett. **77** 1683 (1996); W. Hampel et al., Phys. Lett. **B447** 127 (1999).
- [16] M. Apollonio et al., Phys. Lett. **B466** 415 (1999) and Phys. Lett. **B338**, 383 (1998).
- [17] H.V. Klapdor-Kleingrothaus, H. Pas, and A.Y. Smirnov, hep-ph/0003219. See also M. Czakon, J. Gluza, J. Studnik and M. Zlarlek, hep-ph/0010077.
- [18] Private Communication with T. Ohshima.
- [19] M. Fukugita, Guo-Chin Liu, and N. Sugiyama, Phys. Rev. Lett. **84** 1082 (2000).
- [20] H. Minakata and O. Yasuda, Phys. Rev. **D56**, 1692 (1997); R. Adhikari and G. Rajasekaran, Phys. Rev. **D61**, 031301 (2000); W. Rodejohann, hep-ph/0008044.

FIGURES

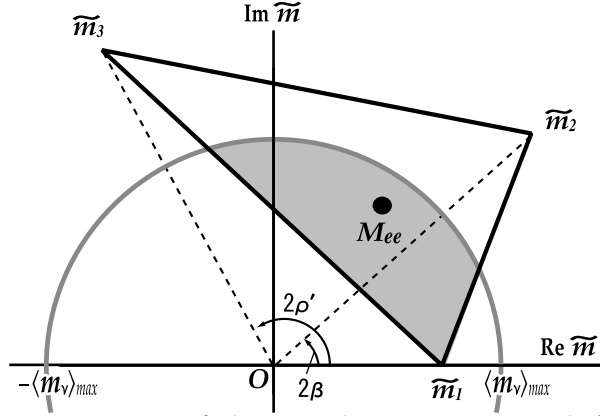


FIG. 1. Graphical representations of the complex mass M_{ee} and CP violating phases. The position of M_{ee} is within the triangle formed by the three points $\widetilde{m}_i (i = 1, 2 \text{ and } 3)$ which are defined in Eq.(2.3). The allowed position of M_{ee} is in the intersection (shaded area) of the inside of this triangle and the inside of the circle of radius $\langle m_\nu \rangle_{max}$ around the origin.

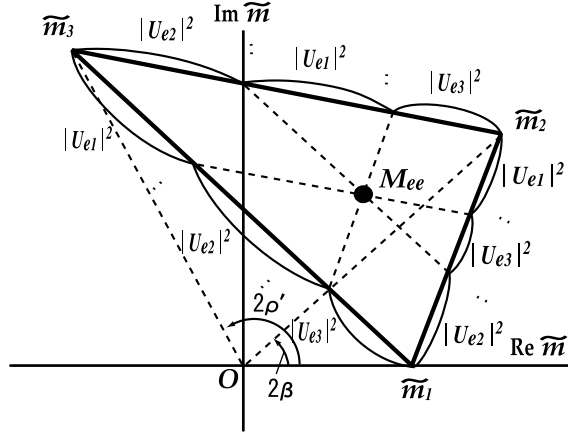


FIG. 2. The relations between the position M_{ee} and $U_{ei} (i = 1, 2 \text{ and } 3)$ components of MNS mixing matrix. The three mixing elements $|U_{ej}|^2 (j = 1, 2 \text{ and } 3)$ indicate the division ratios for the three portions of each side of the triangle which are divided by the parallel lines to the side lines of the triangle passing through M_{ee} .

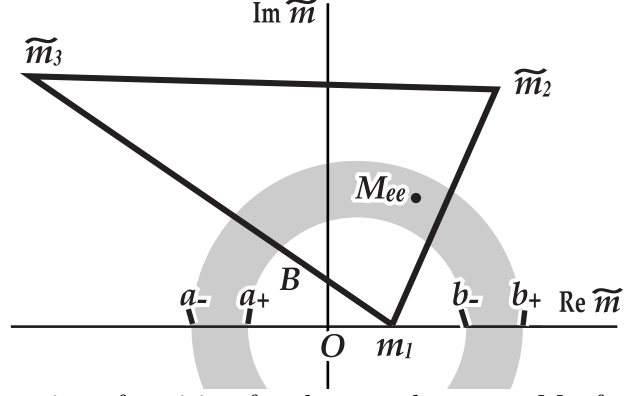


FIG. 3. The allowed region of position for the complex mass M_{ee} from $(\beta\beta)_{0\nu}$ obtained from Eq.(3.2). In this figure, $a_- \equiv |U_{e1}|^2 m_1 - (|U_{e2}|^2 m_2 + |U_{e3}|^2 m_3)$, $a_+ \equiv |U_{e1}|^2 m_1 - ||U_{e2}|^2 m_2 - |U_{e3}|^2 m_3|$, $b_- \equiv |U_{e1}|^2 m_1 + ||U_{e2}|^2 m_2 - |U_{e3}|^2 m_3|$ and $b_+ \equiv |U_{e1}|^2 m_1 + (|U_{e2}|^2 m_2 + |U_{e3}|^2 m_3)$.

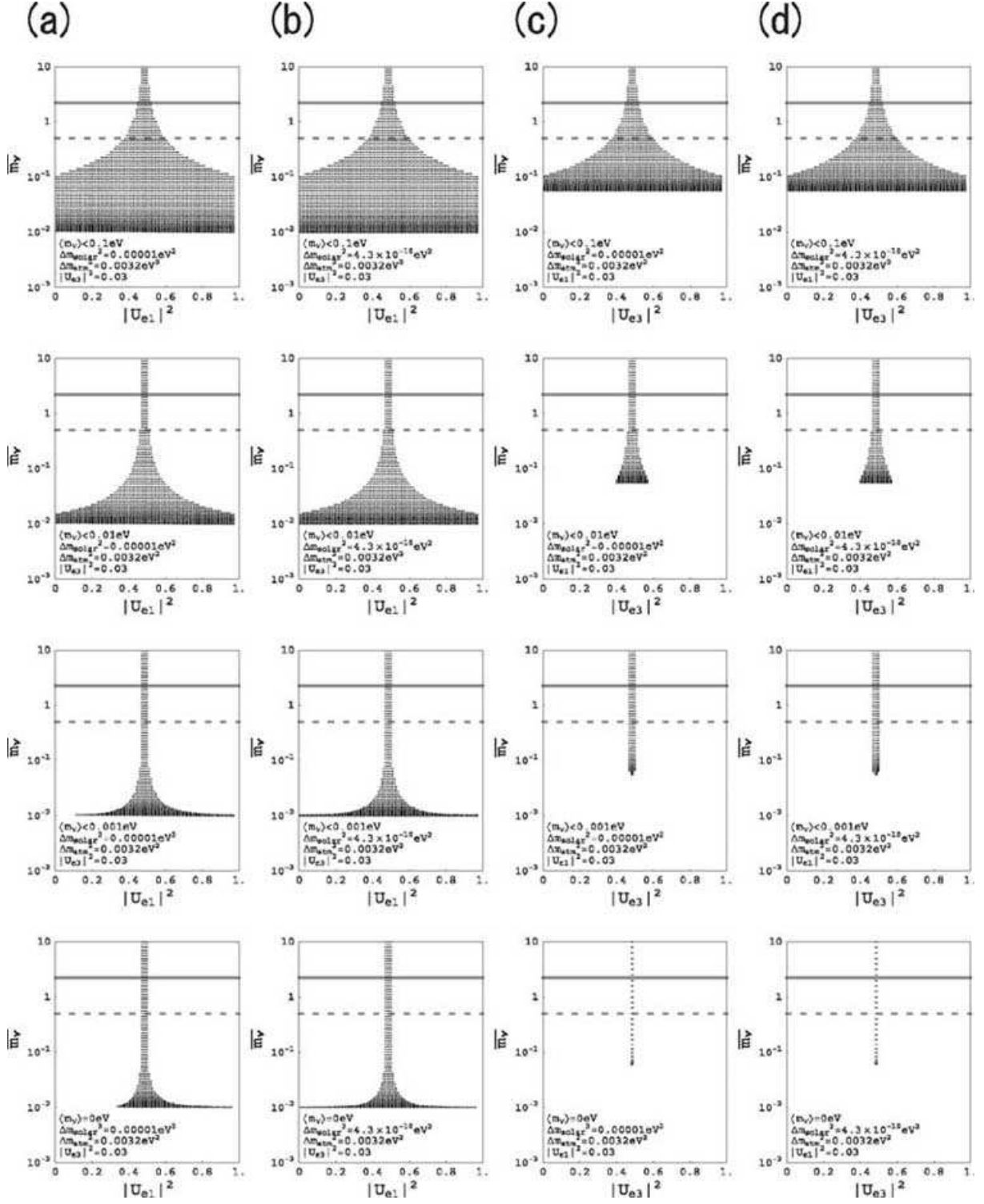


FIG. 4. The allowed regions in the $\overline{m_\nu}$ - $|U_{e1}|^2$ plane for fixed values of $\langle m_\nu \rangle_{max}$, Δm_{solar}^2 , Δm_{atm}^2 , and $|U_{e3}|^2$ in the normal mass hierarchy scenario ((a) and (b)), and in the $\overline{m_\nu}$ - $|U_{e3}|^2$ plane for fixed values of $\langle m_\nu \rangle_{max}$, Δm_{solar}^2 , Δm_{atm}^2 , and $|U_{e1}|^2$ in the inverse mass hierarchy scenario ((c) and (d)). Here we choose $|U_{e3}|^2$ or $|U_{e1}|^2 = 0.03$. The allowed regions change very little when $|U_{e3}|^2$ or $|U_{e1}|^2 < 0.03$. The figures of the first and the second rows are for the MSW and Just So solutions for the solar neutrino problem respectively in the normal mass hierarchy scenario. The third and fourth ones are for the MSW and Just So solutions in the inverse mass hierarchy scenario. The first, second, third, and fourth columns are for $\langle m_\nu \rangle < 0.1$ eV, $\langle m_\nu \rangle < 0.01$ eV, $\langle m_\nu \rangle < 0.001$ eV, and $\langle m_\nu \rangle = 0$ eV, respectively. The gray solid (dotted) line shows the present bound $\overline{m_\nu} < 2.2$ eV by Mainz (the future bound $\overline{m_\nu} < 0.5$ eV) [2].

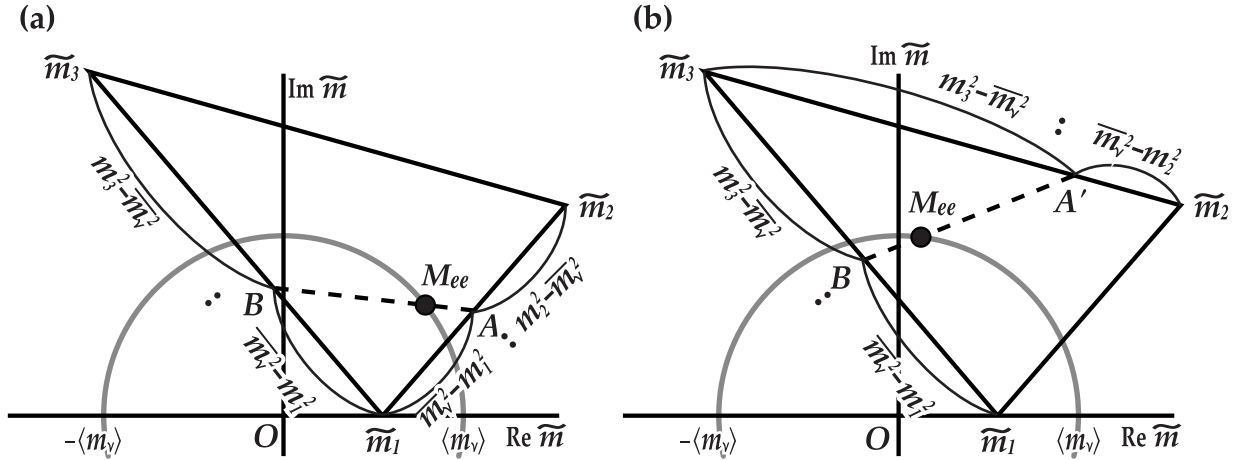


FIG. 5. The allowed position of the complex mass M_{ee} from $(\beta\beta)_{0\nu}$ and the single beta decay.

The position of M_{ee} is restricted to be on the line segment AB in Fig.5(a) for the case $\overline{m_\nu} < m_2$ or $A'B$ in Fig.5(b) for the case $\overline{m_\nu} > m_2$ with given definite values of $\overline{m_\nu}$, m_i , and one free parameter of mixing matrix element.

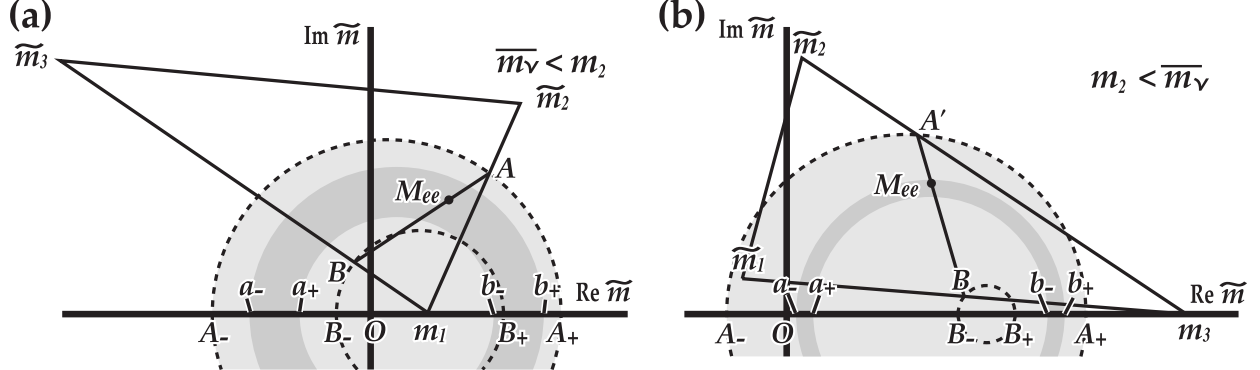


FIG. 6. The allowed region of M_{ee} obtained by making the CP violating phases run freely for the cases in which (a) $\overline{m_\nu} < m_2$ and (b) $\overline{m_\nu} > m_2$. The dark shaded region is the same as the shaded region in Fig.3, in which we move the CP violating phases freely but fix the mixing angles. The light shaded region is the allowed region for the case where mixing matrix elements are also free and M_{ee} can move along the line segment AB or $A'B$, freely. (i.e. All mixing matrix elements are free parameters.) In left-hand side figure (a), $A_- \equiv (m_1 m_2 - \overline{m_\nu}^2) / (m_2 - m_1)$, $A_+ \equiv (m_1 m_2 + \overline{m_\nu}^2) / (m_2 + m_1)$, $B_- \equiv (m_1 m_3 - \overline{m_\nu}^2) / (m_3 - m_1)$ and $B_+ \equiv (m_1 m_3 + \overline{m_\nu}^2) / (m_3 + m_1)$. The right-hand side figure (b) is obtained by exchanging the suffix 3 for 1 in (a). Therefore, $A_- \equiv (-m_2 m_3 + \overline{m_\nu}^2) / (m_3 - m_2)$, $A_+ \equiv (m_2 m_3 + \overline{m_\nu}^2) / (m_3 + m_2)$, $B_- \equiv (-m_1 m_3 + \overline{m_\nu}^2) / (m_3 - m_1)$ and $B_+ \equiv (m_1 m_3 + \overline{m_\nu}^2) / (m_3 + m_1)$.

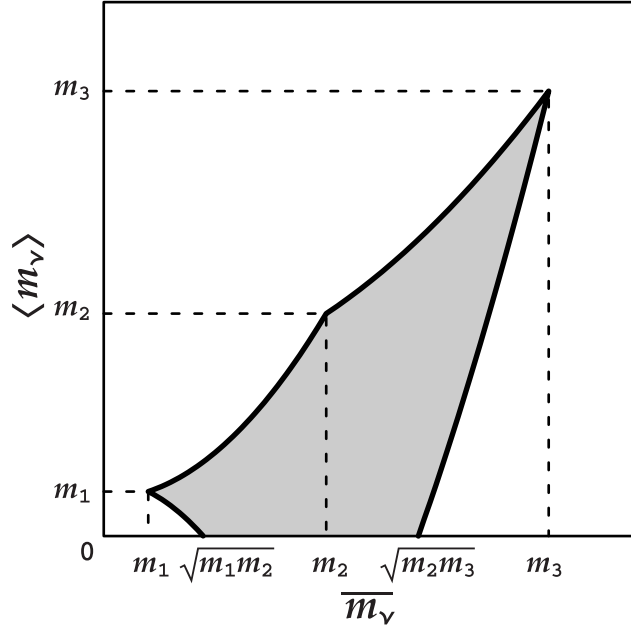


FIG. 7. The allowed region in the $\langle m_\nu \rangle - \overline{m}_\nu$ plane obtained independently of the CP violating phases. This constraint is obtained by considering Fig.6. The boundary curves are given by Eqs. (4.8) and (4.9).

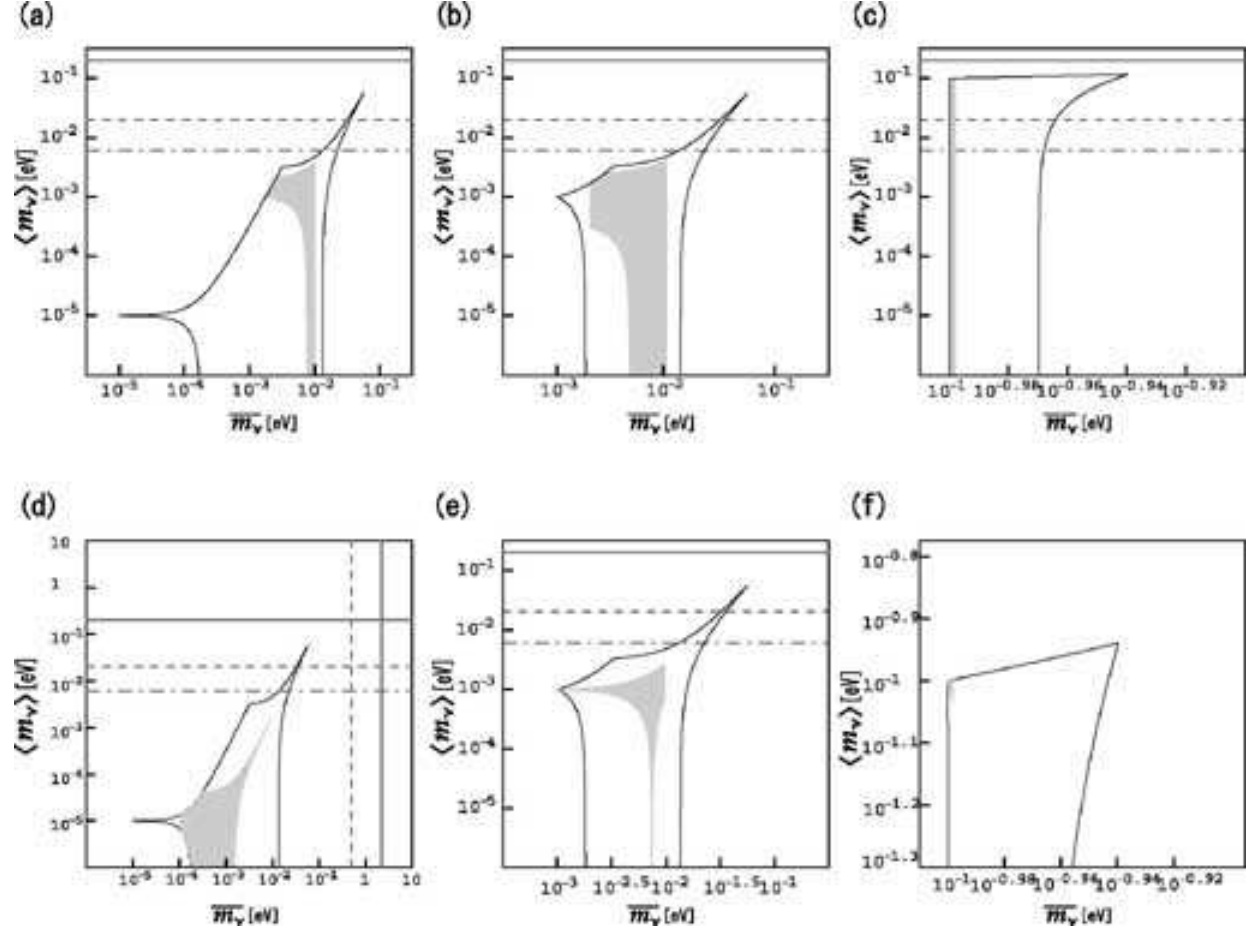


FIG. 8. The allowed region in the $\langle m_\nu \rangle$ - $\overline{m_\nu}$ plane in the normal mass hierarchy obtained independently of the CP violating phases. In this figure the data of the mixing angles are incorporated: $|U_{e3}|^2 < 0.03$ and $0.3 < |U_{e2}|^2 < 0.7$ for LMA-MSW (the upper panels) and $|U_{e3}|^2 < 0.03$, $1 \times 10^{-3} < |U_{e2}|^2 < 1 \times 10^{-2}$ for SMA-MSW (the lower panels). The first, second and third row panels correspond to the case $m_1 = 10^{-5}\text{eV}$, 10^{-3}eV , 10^{-1}eV , respectively. The black solid curve is the boundary of Fig.7. The horizontal lines show the present bound $\langle m_\nu \rangle < 0.2$ eV by Heidelberg-Moscow (gray solid line), the future bounds $\langle m_\nu \rangle < 0.02$ eV by GENIUS I (gray dotted line) and $\langle m_\nu \rangle < 0.006$ eV by GENIUS II (gray dot-dashed line) [6]. The vertical lines show the present bound $\overline{m_\nu} < 2.2\text{eV}$ by Mainz (gray dotted line) and the future bound $\overline{m_\nu} < 0.5\text{eV}$ (gray dotted line)[2], which are on the right out of the panel except for the case (d). In the case of (f), the present limit of $\langle m_\nu \rangle$ is above and GENIUS I, II are below the panel.

(a)

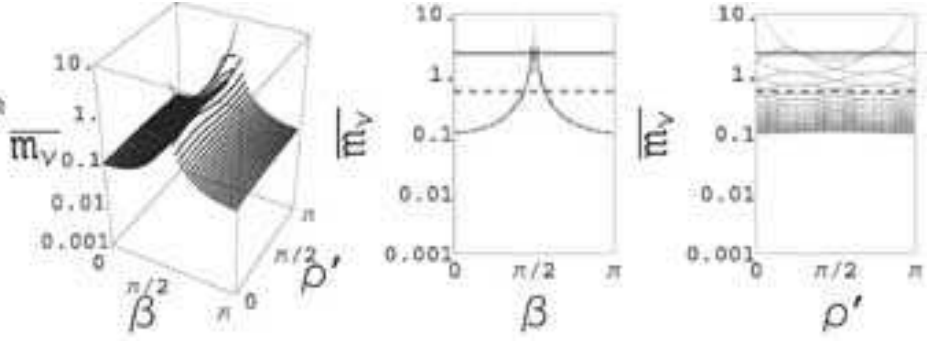
$$\langle m \rangle = 0.1 \text{ eV}$$

$$\Delta m_{\text{solar}}^2 = 1 \times 10^{-5} \text{ eV}^2$$

$$\Delta m_{\text{atm}}^2 = 0.0032 \text{ eV}^2$$

$$|U_{e2}|^2 = 0.5$$

$$|U_{e3}|^2 = 0.03$$



(b)

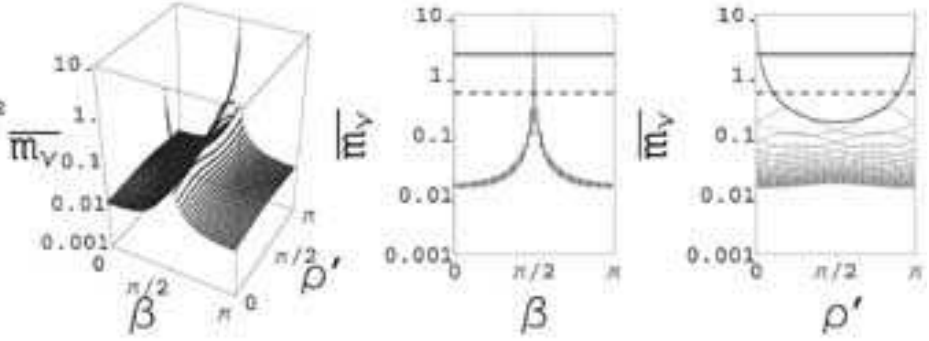
$$\langle m \rangle = 0.01 \text{ eV}$$

$$\Delta m_{\text{solar}}^2 = 1 \times 10^{-5} \text{ eV}^2$$

$$\Delta m_{\text{atm}}^2 = 0.0032 \text{ eV}^2$$

$$|U_{e2}|^2 = 0.5$$

$$|U_{e3}|^2 = 0.03$$



(c)

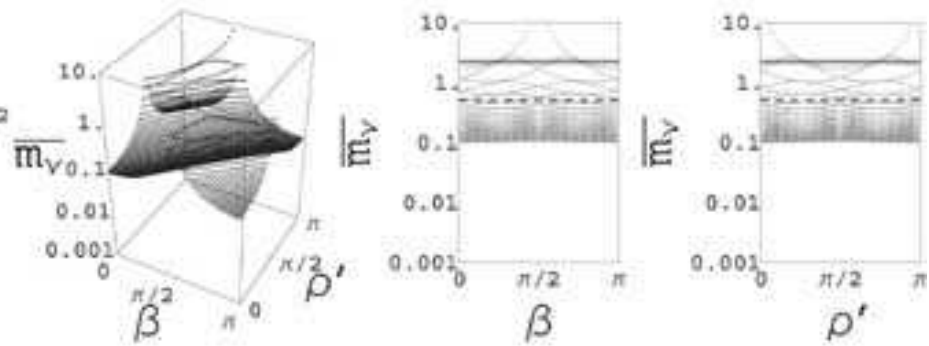
$$\langle m \rangle = 0.1 \text{ eV}$$

$$\Delta m_{\text{solar}}^2 = 1 \times 10^{-5} \text{ eV}^2$$

$$\Delta m_{\text{atm}}^2 = 0.0032 \text{ eV}^2$$

$$|U_{e2}|^2 = 0.5$$

$$|U_{e3}|^2 = 0.03$$



(d)

$$\langle m \rangle = 0.01 \text{ eV}$$

$$\Delta m_{\text{solar}}^2 = 1 \times 10^{-5} \text{ eV}^2$$

$$\Delta m_{\text{atm}}^2 = 0.0032 \text{ eV}^2$$

$$|U_{e2}|^2 = 0.5$$

$$|U_{e3}|^2 = 0.03$$

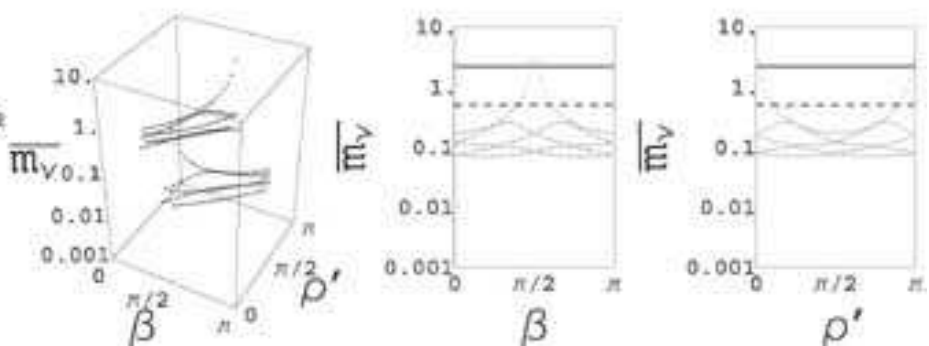


FIG. 9. The allowed region among $\overline{m_\nu}$, CP violating phases β , and ρ' for the LMA-MSW solution for the solar neutrino problem in the normal ((a) and (b)) and inverse ((c) and (d)) neutrino mass hierarchy. We take the following values: $\langle m_\nu \rangle = 0.1$ eV and 0.01 eV and the others are fixed as $|U_{e2}|^2 = 0.5$, $|U_{e3}|^2 = 0.03$, $\Delta m_{solar}^2 = 1 \times 10^{-5} \text{eV}^2$ and $\Delta m_{atm}^2 = 3.2 \times 10^{-3} \text{eV}^2$. The gray solid (dotted) line shows the present bound $\overline{m_\nu} < 2.2 \text{eV}$ by Mainz (the future bound $\overline{m_\nu} < 0.5 \text{eV}$) [2].

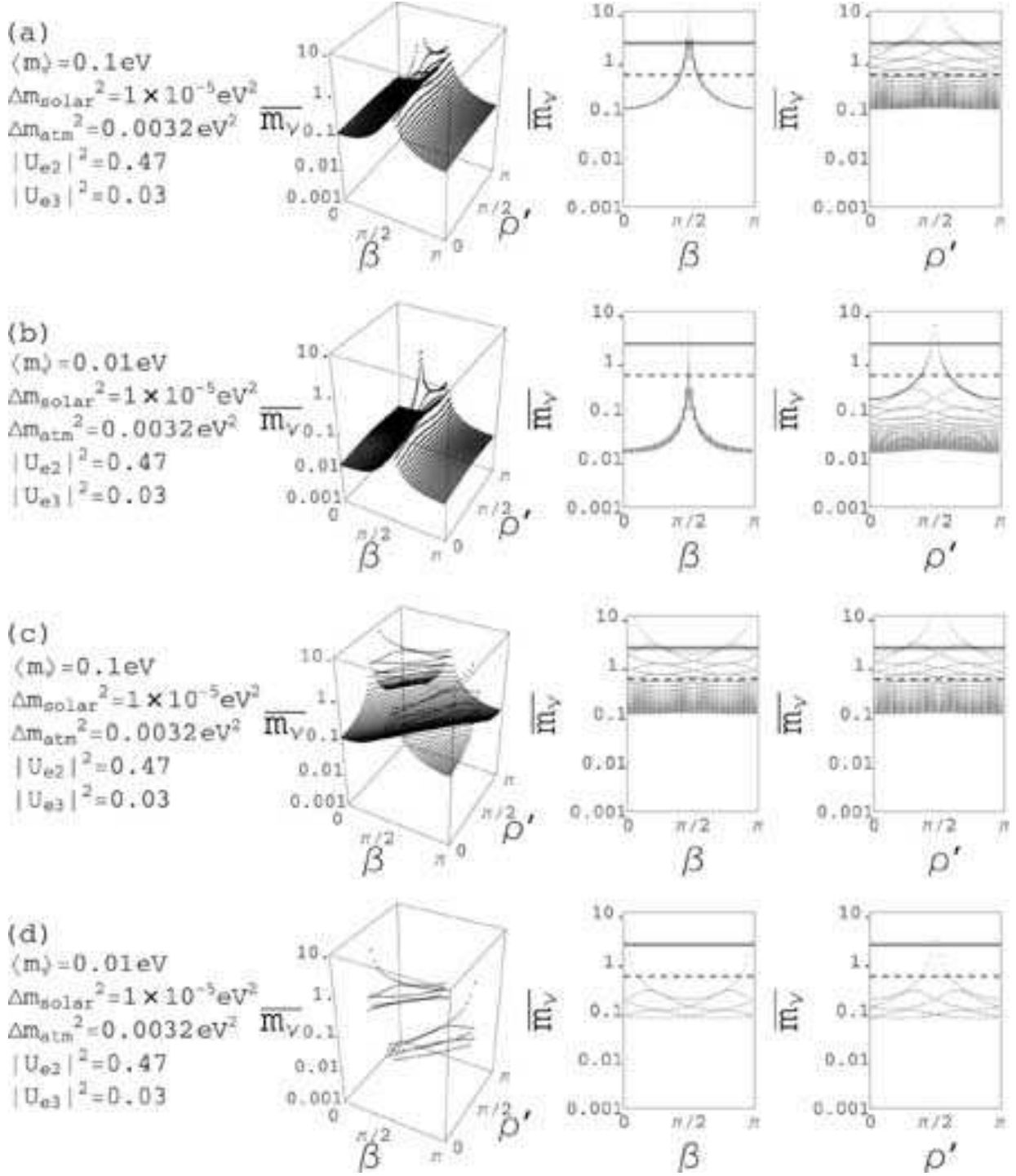


FIG. 10. Same as Fig.9 except for $|U_{e2}|^2 = 0.47$ in place of $|U_{e2}|^2 = 0.5$.